Composite pulses with errant phases

Boyan T. Torosov[1] and Nikolay V. Vitanov[2]
[1]*Institute of Solid State Physics, Bulgarian Academy of Sciences, 72 Tsarigradsko Chaussée, 1784 Sofia, Bulgaria*
[2]*Department of Physics, St Kliment Ohridski University of Sofia, 5 James Bourchier Boulevard, 1164 Sofia, Bulgaria*

(Received 26 April 2019; revised manuscript received 20 May 2019; published 12 August 2019)

Composite pulses—sequences of pulses with well-defined relative phases—are an efficient, robust, and flexible technique for coherent control of quantum systems. Composite sequences can compensate for a variety of experimental errors in the driving field (e.g., in the pulse amplitude, duration, detuning, chirp, etc.) or in the quantum system and its environment (e.g., inhomogeneous broadening, stray electric or magnetic fields, unwanted couplings, etc.). The control parameters are the relative phases between the constituent pulses in the composite sequence, an accurate control over which is required in all composite sequences reported hitherto. In this paper, we introduce two types of composite pulse sequences which, in addition to error compensation in the basic experimental parameters, compensate for systematic errors in the composite phases. In the first type of such composite sequences, which compensate for pulse area errors, relative phase errors of over 10% can be tolerated with reasonably short sequences while maintaining the fidelity above the 99.99% quantum computing benchmark. In the second type of composite sequences, which compensate for simultaneous pulse area and detuning errors, relative phase errors of over 5% can be compensated.

DOI: 10.1103/PhysRevA.100.023410

I. INTRODUCTION

Since their invention in nuclear magnetic resonance (NMR) 40 years ago [1–13] composite pulses have established themselves as a major technique for coherent control of quantum systems. Composite pulses offer a unique combination of ultrahigh accuracy, well below the error threshold in quantum computation (often referred to as 10^{-4}), with robustness to parameter errors similar to adiabatic passage techniques [14]. Moreover, they offer great flexibility in shaping the excitation profile, or even the propagator, in essentially any desired manner—a feature that is not available in any other quantum control method.

In recent years composite pulses have remained as popular a control tool as ever in compensating for systematic field errors in NMR, including traditional applications [15–24], development of new types of composite pulses [25–29], applications to new platforms, e.g., muon spin resonance [30], and quantum computation [31,32]. Moreover, composite pulses have enjoyed significant interest and numerous applications in various fields across quantum physics well beyond NMR. A few representative examples include qubit control in trapped ions [33–39] and neutral atoms [40], high-accuracy optical clocks [41], cold-atom interferometry [42–44], optically dense atomic ensembles [45], singlet-triplet quantum-dots qubits [46–49], triple quantum dots [50,51], nitrogen-vacancy centers in diamond [52], magnetometry [53], optomechanics [54], etc. We also note recent developments toward arbitrary accurate composite pulses [55–57], composite adiabatic passage [58,59] including nonlinearities [60], concatenated composite pulses compensating simultaneous systematic errors [61–63], composite quantum gates [64–70], composite pulses designed using neural-network concepts [71], composite pulses with non-Markovian noise [72], etc.

Curiously, the concept of composite sequences has been well known in polarization optics since the 1940s [73–78], where achromatic wave plates or polarization filters can be constructed by a set of ordinary wave plates with their fast (or slow) polarization axes rotated at specific angles with respect to each other. Recently, the composite idea has been extended to frequency conversion processes in nonlinear optics [79,80].

The composite pulse sequence is a finite train of pulses with well-defined phases, which are used as control parameters in order to compensate for experimental errors or to shape the excitation profile in a desired manner. The most ubiquitous composite sequences are the broadband π pulses, which produce unit transition probability not only for a pulse area $\mathcal{A} = \pi$ and zero detuning $\Delta = 0$, as a single resonant π pulse, but also in some (broad) ranges around these values. Hence a composite π pulse can compensate the pulse area and detuning errors of a single π pulse and make a sequence of imperfect pulses act like an ideal π pulse. Among the broadband composite π pulses, we note those which compensate pulse area errors, detuning errors, and both pulse area and detuning errors [13]. Recently, composite pulses, which compensate experimental errors in any experimental parameter—universal composite pulses—have been introduced and experimentally demonstrated [81]. Composite θ pulses, which produce controlled partial excitation with probability $\sin^2(\theta/2)$, are also available [5,10,82,83] and they have important applications in quantum computation. There are two other types of composite sequences: narrowband [10,84–89] and passband [6–8,10,28,90] composite pulses. Narrowband pulses squeeze the excitation profile inside a narrow range around a certain point in the parameter space and suppress excitation outside of it. Passband pulses combine the features of broadband and narrowband pulses: highly efficient

excitation in a certain parameter range and very low excitation outside.

In all known composite sequences an accurate control of the composite phases has been presumed. Because the underlying physical mechanism of composite pulses is constructive or destructive interference of probability amplitudes, the excitation profile is very sensitive to phase errors. Typically, the relative phase errors must not exceed 0.1–1% for short composite sequences, and even values of less than 0.1% for long sequences are needed to achieve the ultrahigh fidelity required in quantum computation. This requirement restricts the application of composite pulses to physical systems wherein such accuracy is possible. For radio-frequency and microwave driving fields the composite phases are produced by the respective generator and this requirement is usually fulfilled. In the optical domain such accuracy may become a challenge, especially if the phase shifts are produced by off-resonant electric or magnetic pulses via Stark and Zeeman shifts.

In the present paper, we introduce a different type of composite π pulse, which is robust to systematic phase errors of the order of 5–15%, e.g., one to two orders of magnitude larger errors than the existing composite pulses can afford. Thereby these composite pulses resolve the only vulnerability of this powerful quantum control method: the necessity to have very well controlled relative phases between the pulses in the composite sequences. We present two types of such phase-error resilient composite sequences: (i) sequences that deliver double compensation of simultaneous errors in the pulse area and the composite phases, and (ii) sequences that produce triple compensation of simultaneous errors in the pulse area, the detuning and the composite phases.

This paper is organized as follows. In Sec. II we discuss the mathematical details of the derivation of these new composite pulses. In Sec. III the double-compensation sequences are introduced, and the triple-compensation sequences are presented in Sec. IV. Finally, Sec. V wraps up the conclusions.

II. DESCRIPTION OF THE METHOD FOR CORRECTION OF PHASE ERRORS

Here we describe the method for construction of composite pulses that produce excitation profiles which are robust against simultaneous errors in the pulse area and the composite phases (double compensation). Triple compensation is derived similarly and the specifics are elaborated in Sec. IV.

The propagator of a coherently driven two-state quantum system, described by the Hamiltonian $\mathbf{H}(t) = \frac{1}{2}\hbar[\Omega(t)\sigma_x + \Delta(t)\sigma_z]$, is given by the SU(2) matrix

$$\mathbf{U}_0 = \begin{bmatrix} a & b \\ -b^* & a^* \end{bmatrix}, \tag{1}$$

where a and b are the (complex) Cayley-Klein parameters obeying $|a|^2 + |b|^2 = 1$. For exact resonance ($\Delta = 0$), we have $a = \cos(\mathcal{A}/2)$ and $b = -i\sin(\mathcal{A}/2)$, where $\mathcal{A}$ is the temporal pulse area $\mathcal{A} = \int_{t_i}^{t_f} \Omega(t)dt$. For a system starting in state $|1\rangle$, the single-pulse transition probability is $p = |b|^2 = \sin^2(\mathcal{A}/2)$.

A phase shift ϕ imposed on the driving field, $\Omega(t) \to \Omega(t)e^{i\phi}$, is imprinted onto the propagator as

$$\mathbf{U}_\phi = \begin{bmatrix} a & be^{i\phi} \\ -b^*e^{-i\phi} & a^* \end{bmatrix}. \tag{2}$$

Consider a train of N pulses, each with area A_k and phase ϕ_k,

$$(A_1)_{\phi_1}(A_2)_{\phi_2}(A_3)_{\phi_3}\cdots(A_N)_{\phi_N}. \tag{3}$$

In the presence of pulse area errors, we have to replace the nominal pulse areas A_k by the actual pulse areas $\mathcal{A}_k = A_k(1+\alpha)$ $(k = 1, 2, \ldots, N)$, where α is the relative pulse area error. In the presence of phase errors, each nominal phase ϕ_k should be replaced by the actual phase $\varphi_k = \phi_k(1+\epsilon)$ $(k = 1, 2, \ldots, N)$, where ϵ describes the (systematic) phase errors, the compensation of which is our primary concern here. In the presence of pulse area and phase errors, the pulse sequence (3) produces the propagator

$$\mathbf{U}^{(N)} = \mathbf{U}_{\varphi_N}(\mathcal{A}_N)\cdots\mathbf{U}_{\varphi_3}(\mathcal{A}_3)\mathbf{U}_{\varphi_2}(\mathcal{A}_2)\mathbf{U}_{\varphi_1}(\mathcal{A}_1). \tag{4}$$

Yet, for the sake of brevity, in the notation of the composite pulse sequence (3) we shall use the nominal pulse areas A_k and the nominal phases ϕ_k.

In this paper, based on numerical evidence, we consider composite sequences of an odd number $N = 2n+1$ $(n = 1, 2, \ldots)$ of identical pulses, and nominal pulse area $A_k = \pi$ $(k = 1, 2, \ldots, N)$. We also consider symmetric phases, $\phi_k = \phi_{N+1-k}$ $(k = 1, 2, \ldots, n)$. Using the invariance of the transition probability to the addition of the same phase shift to all phases (see Appendix), we set $\phi_1 = \phi_N = 0$. Hence, the phase-error-correcting composite sequences are

$$\Phi N = \pi_0\pi_{\phi_2}\cdots\pi_{\phi_n}\pi_{\phi_{n+1}}\pi_{\phi_n}\cdots\pi_{\phi_2}\pi_0, \tag{5}$$

and the total propagator turns into

$$\mathbf{U}^{(N)} = \mathbf{U}_0(\mathcal{A})\mathbf{U}_{\varphi_2}(\mathcal{A})\cdots\mathbf{U}_{\varphi_{n+1}}(\mathcal{A})\cdots\mathbf{U}_{\varphi_2}(\mathcal{A})\mathbf{U}_0(\mathcal{A}), \tag{6}$$

with $\mathcal{A} = \pi(1+\alpha)$ and

$$\mathbf{U}_\varphi(\mathcal{A}) = \begin{bmatrix} \cos(\mathcal{A}/2) & -i\sin(\mathcal{A}/2)e^{i\varphi} \\ -i\sin(\mathcal{A}/2)e^{-i\varphi} & \cos(\mathcal{A}/2) \end{bmatrix}. \tag{7}$$

We calculate the product in Eq. (6) and expand $U_{11}^{(N)}$ vs α and ϵ at $(\alpha = 0, \epsilon = 0)$. Then we set to zero as many terms as possible in order to obtain a robust excitation profile. If we denote the (j, l)th multivariate coefficient in the power series as

$$s_{jl} = \frac{\alpha^j\epsilon^l}{j!l!}\left(\frac{\partial^{j+l}U_{11}^{(N)}}{\partial\alpha^j\partial\epsilon^l}\right)_{\alpha=0,\epsilon=0}, \tag{8}$$

one can easily verify that because of the chosen symmetry in the phases and pulse areas of the composite sequence, we have

$$s_{jl} \equiv 0 \quad \text{(for all even } j\text{)}. \tag{9}$$

Hence the first nonzero derivatives with respect to the pulse area error α are the first derivatives $(j = 1)$, then the third derivatives $(j = 3)$, etc. With respect to the phase error ϵ all derivatives are generally nonzero. Because the primary objective of the composite pulses is the compensation of pulse area (and detuning) errors, we limit ourselves to the cancellation of the low-order (up to first or second) derivatives with respect to the phase error ϵ, which already provides

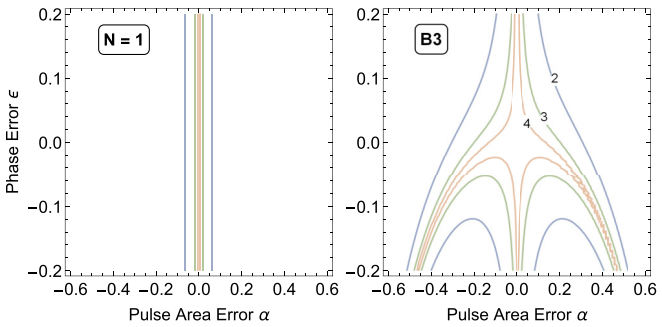

FIG. 1. Transition probability vs pulse area deviation α and phase error ϵ for a single pulse (left) and the B3 sequence (11) (right). The numbers $m = 2, 3, 4$ on the contours correspond to probability levels of $1–10^{-m}$.

significant improvement over the existing composite pulses. Generally, for $N = 2n + 1$ pulses we have n different phases, with which we can nullify n different derivatives.

III. COMPENSATION OF PULSE AREA AND PHASE ERRORS

A. Composite sequences of three pulses

We first consider a sequence of three pulses. We calculate the product in Eq. (6) and expand $U_{11}^{(3)}$ at $\alpha = 0$ and $\epsilon = 0$. We obtain for the first nonzero coefficient in the expansion

$$s_{10} = \alpha\frac{\pi}{2}[1 + 2\cos(\phi_2)]. \tag{10}$$

We can nullify this coefficient by setting $\phi_2 = 2\pi/3$. The resulting composite sequence

$$B3 = \pi_0\pi_{\frac{2}{3}\pi}\pi_0 \tag{11}$$

is one of the best known broadband composite pulses for compensation of pulse area errors [2]. Hence we do not obtain additional compensation in the phase error because of the absence of free phases. (Letting ϕ_3 be nonzero does not help annul s_{11}.) Longer sequences with $N > 3$, studied below, do allow such compensation.

In Fig. 1 the transition probability for the composite sequence B3 is plotted as a function of the pulse area error α and the systematic error ϵ in the phases. We also plot the excitation profile of a single pulse ($N = 1$), which is insensitive to systematic phase error (as far as the transition probability is concerned), but it lacks compensation in the pulse area.

B. Composite sequences of five pulses

We now consider a sequence of five pulses. Similar to the $N = 3$ case, we calculate the product in Eq. (6) and expand $U_{11}^{(5)}$ at $(\alpha = 0, \epsilon = 0)$. We obtain for the first nonzero coefficients in the expansion the expressions

$$s_{10} = -\frac{\pi}{2}\alpha[1 + 2\cos(\phi_2 - \phi_3) + 2\cos(2\phi_2 - \phi_3)], \tag{12a}$$

$$s_{11} = \pi\alpha\epsilon[(\phi_2 - \phi_3)\sin(\phi_2 - \phi_3) + (2\phi_2 - \phi_3)\sin(2\phi_2 - \phi_3)]. \tag{12b}$$

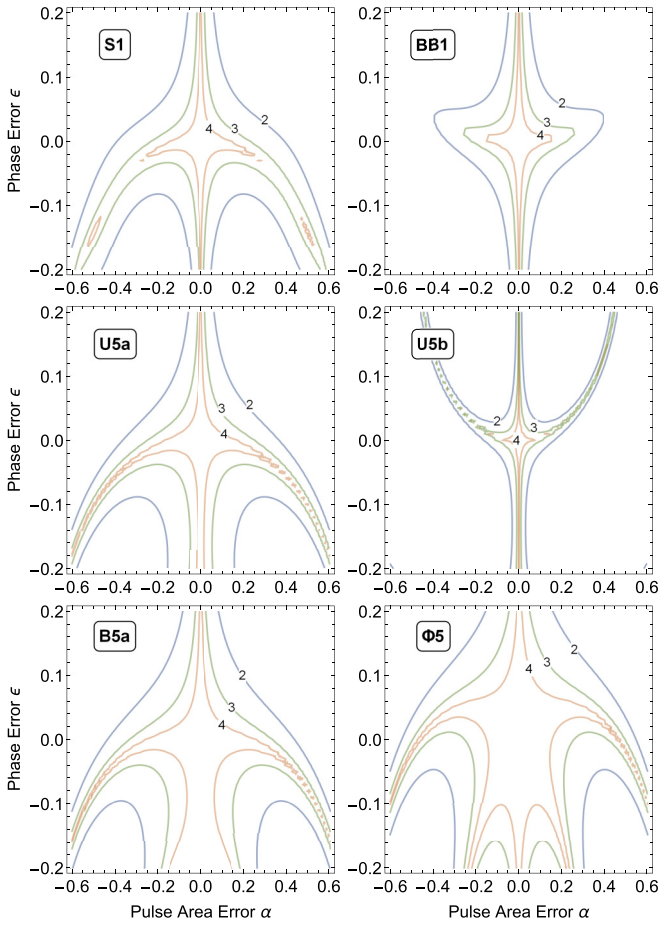

FIG. 2. Transition probability vs pulse area deviation α and phase error ϵ for the six different composite sequences of five π pulses given by Eqs. (13) and (14) (denoted by the labels in the frames). The numbers $m = 2, 3, 4$ on the contours correspond to probability levels of $1–10^{-m}$.

The set of equations $s_{10} = 0$ and $s_{11} = 0$ does not have an analytic solution because the latter of these is transcendental. The values of ϕ_2 and ϕ_3, which nullify s_{10} and s_{11}, can be found numerically. One of the solutions is (approximately) $\phi_2 = 0.743\pi$, $\phi_3 = 0.395\pi$, and hence the composite sequence reads

$$\Phi 5 = \pi_0\pi_{0.743\pi}\pi_{0.395\pi}\pi_{0.743\pi}\pi_0. \tag{13}$$

This composite sequence eliminates errors in the pulse area up to order $O(\alpha^2)$ and in the phases up to order $O(\epsilon^1)$.

In Fig. 2 the transition probability generated by the composite sequence $\Phi 5$ is plotted as a function of the pulse area error α and the systematic error ϵ in the phases, and compared to five well-known previous five-pulse sequences with the same nominal total pulse area 5π,

$$\mathrm{S1} = \pi_0\pi_0\pi_{\frac{2}{3}\pi}\pi_{\frac{1}{3}\pi}\pi_{\frac{2}{3}\pi}, \tag{14a}$$

$$\mathrm{BB1} = \pi_0\pi_\chi\pi_{3\chi}\pi_{3\chi}\pi_\chi, \tag{14b}$$

$$\mathrm{U5}a = \pi_0\pi_{\frac{5}{6}\pi}\pi_{\frac{1}{3}\pi}\pi_{\frac{5}{6}\pi}\pi_0, \tag{14c}$$

$$\mathrm{U5}b = \pi_0\pi_{\frac{11}{6}\pi}\pi_{\frac{1}{3}\pi}\pi_{\frac{11}{6}\pi}\pi_0, \tag{14d}$$

$$\mathrm{B5}a = \pi_0\pi_{\frac{4}{5}\pi}\pi_{\frac{2}{5}\pi}\pi_{\frac{4}{5}\pi}\pi_0, \tag{14e}$$

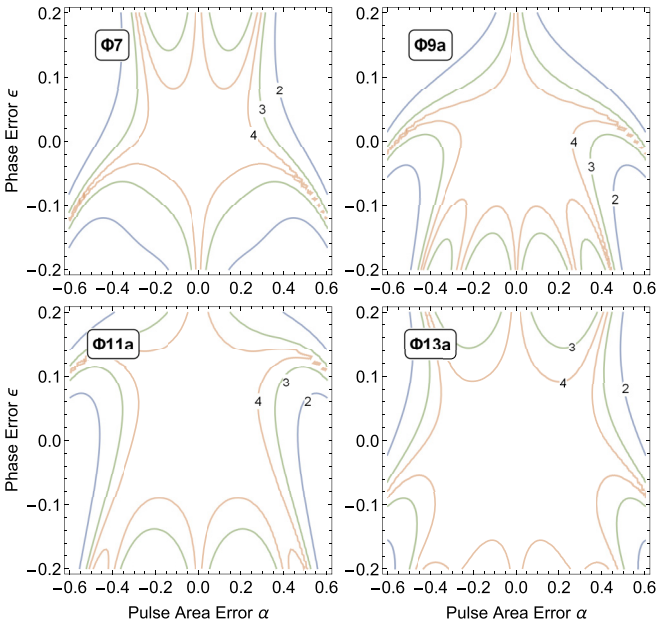

FIG. 3. Transition probability vs pulse area deviation α and phase error ϵ for phase-error-compensating sequences with $N = 7, 9, 11, 13$ pulses. The phases are given in Table I. The numbers $m = 2, 3, 4$ on the contours correspond to probability levels of $1–10^{-m}$.

with $\chi = \cos^{-1}(-1/4) \approx 0.5804\pi \approx 104.5^\circ$. Here S1 is the five-pulse sequence of Tycko and Pines [84], BB1 is the five-pulse sequence of Wimperis [10], U5a [55,81] and U5b [81,84] are universal composite pulses (designed to compensate errors in all experimental parameters but the phases), and B5a is the five-pulse sequence of Ref. [55]. Obviously, the phase-compensating composite pulse $\Phi 5$ provides an ultra-accurate transition probability ($p > 99.99\%$) over a much broader region than the other composite pulses. Note that the composite pulse B5a is fairly resilient to phase errors, although not as much as the dedicated phase-error-correcting composite pulse $\Phi 5$. The reason is that the values of its phases are not too far from the ones of $\Phi 5$, see Eqs. (13) and (14e).

C. Longer composite sequences

We continue with a sequence of seven pulses, which presents us three phases to be used as free control parameters. We choose the nonzero coefficients, which we want to nullify, to be s_{10}, s_{11}, and s_{30}. The explicit expressions for these coefficients are too cumbersome to be presented here, but their numeric cancellation is straightforward. In such a way, we obtain numerous solutions for the phases, one of which is $\phi_2 = 0.591\pi$, $\phi_3 = -0.307\pi$ and, $\phi_4 = -0.575\pi$. Hence the corresponding seven-pulse composite sequence reads

$$\Phi 7 = \pi_0 \pi_{0.591\pi} \pi_{-0.307\pi} \pi_{-0.575\pi} \pi_{-0.307\pi} \pi_{0.591\pi} \pi_0. \quad (15)$$

Figure 3 (top left) shows the excitation profiles of this phase-compensating composite sequence. Clearly, the high-probability area is larger than for the $\Phi 5$ sequence in Fig. 2.

For longer sequences we can proceed in a similar manner. The additional free phases allow us to cancel higher-order terms s_{jl}. Representative examples of the composite sequences derived in this manner and the corresponding null s_{jl} terms are presented in Table I. In Fig. 3 we plot the excitation profiles for sequences of length $N = 7, 9, 11, 13$. A systematic improvement of the excitation profile is observed as the length of the composite sequences increases, with the tolerance ranges exceeding 40% for pulse area errors and 10% for phase errors.

TABLE I. Nullified s_{jl} terms and the corresponding nominal phases for phase-error-compensating composite sequences with different length N. All phases are in units π. Note that all terms s_{jl} with even j are zero, see Eq. (9), and hence they are not listed here.

ΦN	Null terms and composite phases
$\Phi 5$	(s_{10}, s_{11})
	(0, 0.7433, 0.3951, 0.7433, 0)
$\Phi 7$	(s_{10}, s_{11}, s_{30})
	(0, 0.5906, −0.3069, −0.5749, −0.3069, 0.5906, 0)
$\Phi 9a$	$(s_{10}, s_{11}, s_{12}, s_{30})$
	(0, 0.8095, 0.5444, 1.1007, 0.1715, 1.1007, 0.5444, 0.8095, 0)
$\Phi 9b$	$(s_{10}, s_{11}, s_{30}, s_{31})$
	(0, 1.4073, 0.2688, 0.6144, 1.6587, 0.6144, 0.2688, 1.4073, 0)
$\Phi 11a$	$(s_{10}, s_{11}, s_{30}, s_{31}, s_{50})$
	(0,0.6713,0.3049,1.0965,0.7176,0.0956,
	0.7176, 1.0965, 0.3049, 0.6713, 0)
$\Phi 11b$	$(s_{10}, s_{11}, s_{12}, s_{30}, s_{31})$
	(0, 0.6934, 0.3176, 1.1303, 0.7420, 0.1010,
	0.7420, 1.1303, 0.3176, 0.6934, 0)
$\Phi 13a$	$(s_{10}, s_{11}, s_{30}, s_{31}, s_{50}, s_{51})$
	(0, 0.8097, 0.2288, −0.0720, −0.9158, −0.1132, 0.8688,
	−0.1132, −0.9158, −0.0720, 0.2288, 0.8097, 0)
$\Phi 13b$	$(s_{10}, s_{11}, s_{12}, s_{30}, s_{31}, s_{32})$
	(0, 0.8150, 0.2523, 0.6393, −0.2552, −0.4568, 0.2744)
	−0.4568, −0.2552, 0.6393, 0.2523, 0.8150, 0)
$\Phi 13c$	$(s_{10}, s_{11}, s_{12}, s_{30}, s_{31}, s_{50})$
	(0, 0.7639, 0.1842, −0.1071, −0.8840, −0.0756, 0.8432
	−0.0756, −0.8840, −0.1071, 0.1842, 0.7639, 0)

D. Discussion

It is important to note that in the absence of phase errors ($\epsilon = 0$) different composite pulses can produce the same excitation profile due to the invariance of the transition probability to various transformations of the phases, see Appendix. However, in the presence of phase errors, the picture changes drastically. For example, we cannot add or subtract phases 2π to or from any chosen phase because the phase error ϵ multiplies the phases ϕ_k and $\phi_k \pm 2\pi$ differently and hence these different phases will lead to different excitation profiles.

To this end, here we have restricted ourselves to solutions for the composite phases in the ranges $[0, 2\pi]$ or $[-\pi, \pi]$. For some of the presented composite sequences there exist other sequences of the same length which produce slightly better (i.e., broader) profiles which, however, have phases lying outside these ranges. For example, the seven-pulse sequence with phases $(\phi_2, \phi_3, \phi_4) = (1.1703, 1.4334, 2.9010)\pi$ produces a slightly broader profile than the $\Phi 7$ sequence presented here. We have deliberately omitted these other sequences because

the presented sequences already produce significant phase-error compensation, and also to avoid ambiguity in experimental implementation.

Indeed, if the phase shifts are created by electric or magnetic fields as time-integrated Stark or Zeeman shifts then phases ϕ and $\phi \pm 2\pi$ are physically different and it makes sense to consider the respective composite sequences as different. It is less obvious if phases ϕ and $\phi \pm 2\pi$ can be physically different if created by other mechanisms, e.g., by a microwave generator or an acousto-optical modulator. Therefore, to avoid ambiguity, we have presented only composite sequences with phases in ranges of length 2π, i.e., $(0, 2\pi)$ or $(-\pi, \pi)$. It is important that any experimental realization of our sequences should consider this argument and should use the phases as reported here.

IV. COMPENSATION OF PULSE AREA, DETUNING, AND PHASE ERRORS

We can apply the idea of phase-error-compensating composite pulses to produce sequences which compensate errors in more than one parameter. The derivation of the phases is done in a way much similar to the one described in Sec. II. For instance, to derive sequences that are insensitive to errors in the Rabi frequency, the detuning, and the composite phases, we proceed as follows. First, we should specify the pulse shape in order to obtain the explicit formula for the single-pulse propagator. In our derivation, we assume rectangular pulses. Then we calculate the total propagator by taking the product of the constituent propagators. Next we calculate the multivariate coefficients in the expansion of the total propagator vs the Rabi frequency, the detuning, and the phase error, at the point of perfect population transfer. Finally, we cancel as many of these derivative terms as possible.

We call these composite pulses *triple compensating* and denote them with TN. For instance, the anagram composite sequence of nine rectangular pulses,

$$\mathrm{T9} = \pi_0 \pi_{\phi_2} \pi_{\phi_3} \pi_{\phi_4} \pi_{\phi_5} \pi_{\phi_4} \pi_{\phi_3} \pi_{\phi_2} \pi_0, \tag{16}$$

with phases

$$\phi_2 = 1.348\pi,\ \phi_3 = 1.257\pi,\ \phi_4 = 0.166\pi,\ \phi_5 = 0.167\pi, \tag{17}$$

is robust against errors in the Rabi frequency, the detuning, and the composite phases. In Fig. 4 we compare the transition probabilities of this composite pulse (right column) with the transition probability, produced by the nine-pulse universal composite sequence U9, derived in Ref. [81] (left column), which has the same form as Eq. (16) but with the phases

$$\phi_2 = 0.635\pi,\ \phi_3 = 1.35\pi,\ \phi_4 = 0.553\pi,\ \phi_5 = 0.297\pi. \tag{18}$$

As seen in the figure, with attention to the 99.99% contour (label 4), the universal sequence U9 produces a more robust excitation profile in the absence of phase errors (top frames), but when phase errors are present, the phase-compensating sequence T9 outperforms the universal sequence U9.

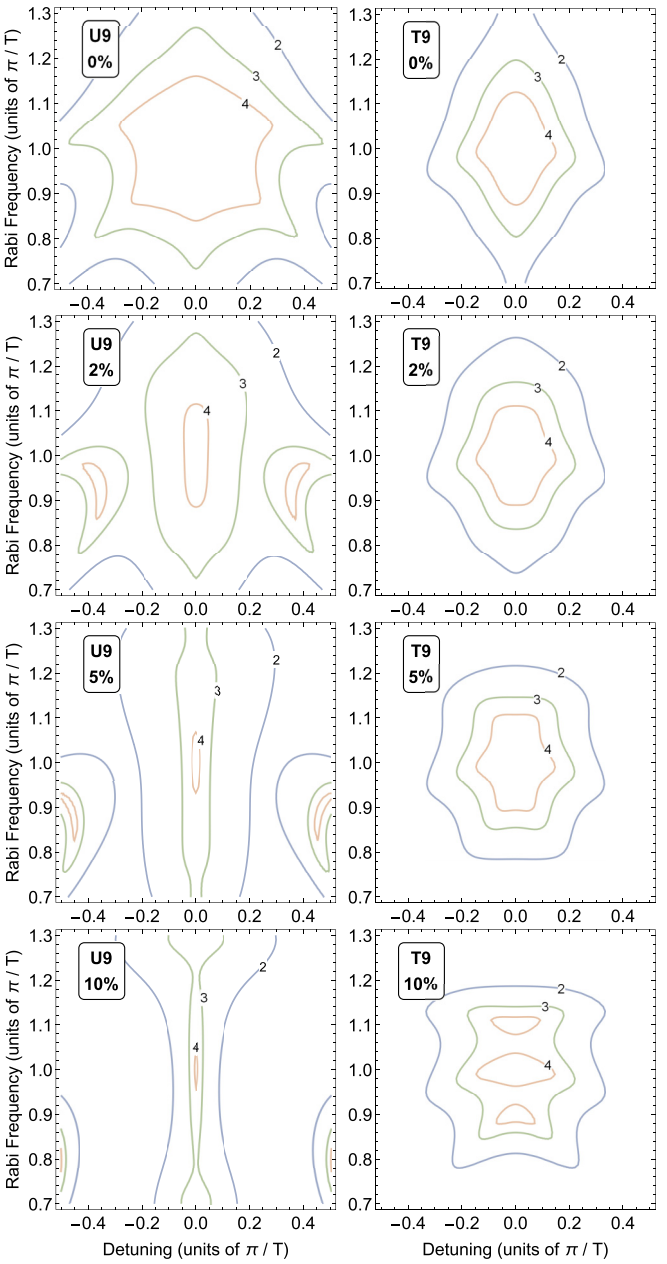

FIG. 4. Transition probability vs Rabi frequency and detuning for composite sequences of nine rectangular pulses. The left column shows the excitation profile for the universal sequence U9 (16) with the phases of Eq. (18) [81], while the right column shows the profiles for the phase-error-corrected sequence T9 with the phases of Eq. (17). The error in the phases is 0%, 2%, 5%, and 10%, from top to bottom.

We have derived composite phases of sequences of up to 11 constituent pulses. The explicit values of these phases are given in Table II. The transition probabilities of these composite pulses are displayed in Fig. 5, where we have used the phases with the label "a" from Table II for each sequence. As the figure shows, efficient compensation of systematic phase errors of up to 5% is achieved in all cases. As the sequences get longer, the high-fidelity domains expand, as expected.

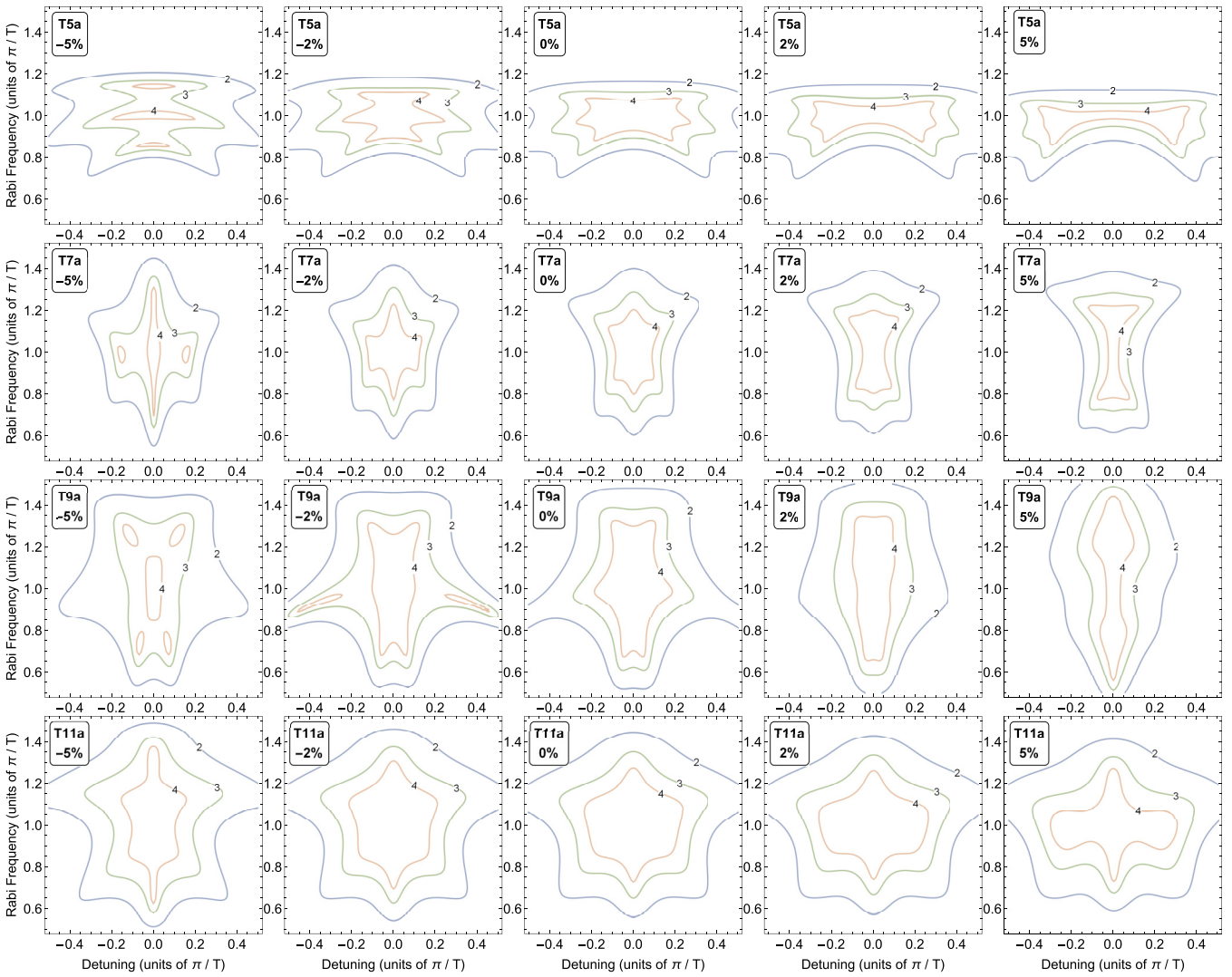

FIG. 5. Transition probability vs Rabi frequency and detuning for triple-compensating composite sequences of five, seven, nine, and eleven rectangular pulses. The error in the phases is 0%, ±2%, ±5%, as labeled.

V. DISCUSSION AND CONCLUSIONS

In the present work we presented an approach to build composite pulses, which are insensitive to systematic errors in the composite phases. We have shown explicit results for sequences of up to 13 pulses, with simultaneous compensation of pulse area and phase errors, but these results can be readily extended to a larger number of pulses, e.g., by concatenation. We have also presented triple compensation of errors in the pulse area, the frequency detuning, and the phases. These phase-error-corrected composite sequences have the potential to eliminate the main limitation of the composite pulses: the requirement for accurate phase control. They should make it possible to extend the application of this powerful and flexible technique to physical platforms wherein accurate phase control is difficult or impossible.

One possible application of the proposed phase-compensating composite pulses is in situations when the composite phases are generated by electric or magnetic fields via AC Stark or Zeeman shifts. For instance, the phase shift generated by a far-off resonant field is $\int_{t_i}^{t_f} \Omega^2/(4\Delta)dt$ if first-order adiabatic elimination is considered. Higher orders have been derived in [91]. Therefore, the phase is proportional to a certain area (an integral), and the error is naturally proportional to the phase. The derived phases can be also useful in implementations of the recently proposed generalization of the composite concept to detuning pulses [92], in which a sequence of detuning pulses is used, with the areas of these pulses being the control parameters. Another application of these phase-error resilient composite sequences could be for achromatic devices for frequency conversion in nonlinear optics [79,80]. There the composite approach is implemented by using nonlinear crystals of different materials and different thicknesses: alternating thick slabs of one material used as analogs of π pulses, and thin slabs of another material used for the phase jumps (via controlled phase mismatch). Systematic errors in the composite phases occur naturally because the phases are proportional to the thickness of the corresponding slabs and scale differently for different frequencies.

We note that in this work we only study systematic errors in the phases. The more general situation of independent errors

TABLE II. Nominal phases for triple-compensating composite sequences with different number of pulses N. All phases are in units π.

TN	Composite phases
T5a	$(0, \frac{1}{6}, -\frac{1}{3}, \frac{1}{6}, 0)$
T5b	$(0, \frac{5}{6}, \frac{1}{3}, \frac{5}{6}, 0)$
T5c	$(0, \frac{7}{6}, \frac{5}{3}, \frac{7}{6}, 0)$
T7a	$(0, 0.8626, \frac{1}{3}, -0.8626, \frac{1}{3}, 0.8626, 0)$
T7b	$(0, 0.7924, \frac{1}{3}, -0.7924, \frac{1}{3}, 0.7924, 0)$
T7c	$(0, 0.4639, \frac{1}{3}, -0.4639, \frac{1}{3}, 0.4639, 0)$
T9a	(0,1.0979,1.3797,0.9631,0.1139, 0.9631, 1.3797, 1.0979, 0)
T9b	(0, 1.3482, 1.2567, 0.1663, 0.1673, 0.1663, 1.2567, 1.3482, 0)
T9c	(0,0.4765,1.3853,0.7006,0.4038, 0.7006, 1.3853, 0.4765, 0)
T9d	(0,0.8712,0.5542,1.2371,0.3424, 1.2371, 0.5542, 0.8712, 0)
T11a	(0, 0.6965, 0.1551, 0.3586, 0.7252, 1.4409, 0.7252, 0.3586, 0.1551, 0.6965, 0)
T11b	(0, 0.8750, 0.5264, 1.3863, 0.5052, 1.2364, 0.5052, 1.3863, 0.5264, 0.8750, 0)
T11c	(0, 0.6179, 0.0723, 0.2972, 0.5752, 1.2186, 0.5752, 0.2972, 0.0723, 0.6179, 0)
T11d	(0, 0.5738, −0.2390, −0.3017, 0.3330, −0.1340, 0.3330, −0.3017, −0.2390, 0.5738, 0)

in the phases is not considered and is left as a potential future project. As such, the present work can be considered useful in physical systems, where the phase shifts may have proportional errors, as the ones described above. Nevertheless, even if the phases are generated by radio-frequency and microwave generators, electro-optic or acousto-optic modulators, one might still want to use the proposed method. This is because even in such very well controlled devices, the generated phases might still contain some systematic error. The reason is that a phase jump in the field never occurs instantly but it takes some (short) time, which, depending on the device, can take a fraction of a microsecond or less. The jump is always followed by a transient interference effect visible as small damped oscillations. The amplitude of this transient effect is proportional to the size of the phase jump (positive or negative) and hence the resulting phase error is proportional to the phase, e.g., it is systematic.

ACKNOWLEDGMENTS

The authors acknowledge useful discussions with Andon Rangelov and Patrick Cheinet. This work is supported by the European Commission's Horizon-2020 Flagship on Quantum Technologies Project No. 820314 (MicroQC).

APPENDIX: NONEQUIVALENCE OF COMPOSITE PULSES IN THE PRESENCE OF PHASE ERRORS

In the absence of phase error ($\epsilon = 0$) different composite pulses can produce the same excitation profile due to the

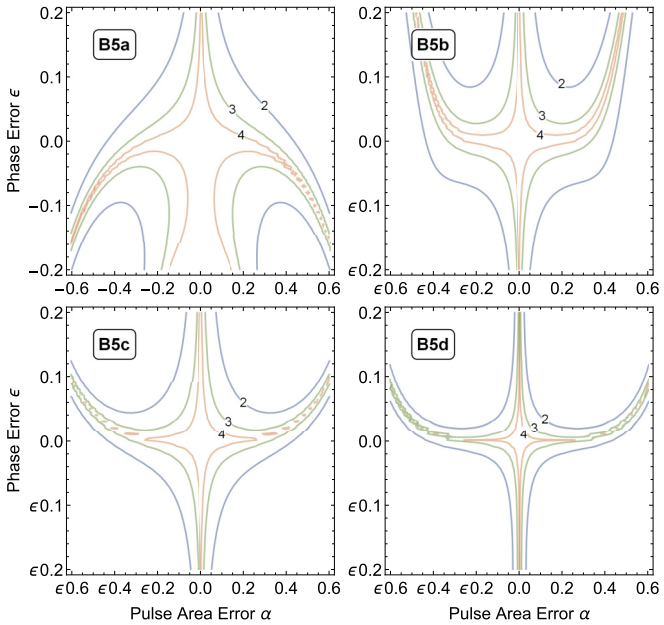

FIG. 6. Transition probability vs pulse area deviation α and phase error ϵ for the four different B5 sequences of Eq. (A3). The numbers $m = 2, 3, 4$ on the contours correspond to probability levels of $1–10^{-m}$.

invariance of the transition probability to various transformations of the phases [83]. Examples of population-preserving transformations are (i) the simultaneous sign flip of all composite phases, $\{-\phi_1, -\phi_2, \ldots -\phi_N\}$; (ii) the addition or subtraction of arbitrary integer multiples of 2π to any composite phase, $\{\phi_1 + 2k_1\pi, \phi_2 + 2k_2\pi, \ldots \phi_N + 2k_N\pi\}$, where k_j are arbitrary integers; (iii) the application of the composite sequence in the reverse order, $\{\phi_N, \phi_{N-1}, \ldots \phi_1\}$; (iv) the addition of the same phase shift, e.g., ϕ_0, to all phases in the sequence. Given a composite pulse sequence, these four features allow one to construct other composite sequences, which deliver the same transition probability. In addition, because the composite phases are derived from a set of trigonometric equations, there are multiple solutions which cannot be obtained from each other by using the above operations but still deliver the same transition probability.

For example, the symmetric composite sequences Bn of Ref. [55], which are of type (5), with phases

$$\phi_k = \frac{k(k-1)n}{N}\pi \quad (k = 1, 2, \ldots, N), \tag{A1a}$$

produce the same excitation profiles as the pulse sequence with the phases

$$\phi_k = \frac{k(k-1)}{N}\pi \quad (k = 1, 2, \ldots, N). \tag{A1b}$$

For $N = 3$ pulses, both Eqs. (A1a) and (A1b) give the well-known sequence (11) [2,55]. By inverting the sign of the second phase and adding 2π we find another equivalent sequence,

$$\pi_0\pi_{\frac{4}{3}\pi}\pi_0. \tag{A2}$$

For $N = 5$ pulses, Eqs. (A1a) and (A1b) produce the two sequences [55]

$$\mathrm{B5}a = \pi_0\pi_{\frac{4}{5}\pi}\pi_{\frac{2}{5}\pi}\pi_{\frac{4}{5}\pi}\pi_0, \tag{A3a}$$

$$\mathrm{B5}b = \pi_0\pi_{\frac{2}{5}\pi}\pi_{\frac{6}{5}\pi}\pi_{\frac{2}{5}\pi}\pi_0. \tag{A3b}$$

Using the transformations described above we can generate two other sequences,

$$\mathrm{B5}c = \pi_0\pi_{\frac{6}{5}\pi}\pi_{\frac{8}{5}\pi}\pi_{\frac{6}{5}\pi}\pi_0, \tag{A3c}$$

$$\mathrm{B5}d = \pi_0\pi_{\frac{8}{5}\pi}\pi_{\frac{4}{5}\pi}\pi_{\frac{8}{5}\pi}\pi_0. \tag{A3d}$$

All four of these sequences produce the same transition probability in the absence of phase errors. In addition we can add or subtract multiples of 2π to or from any phase in the above sequences and generate infinitely many equivalent sequences.

However, in the presence of phase errors, the picture changes drastically. The symmetry properties (i) and (iv) listed above still stand as well as property (iii), which is irrelevant for our symmetric sequences (5). However, property (ii) is not valid any more because the phase error ϵ multiplies the phases. Then the replacement $\phi_k \to \phi_k \pm 2\pi$ of any phase will lead to a different excitation profile. For example, Fig. 6 shows the transition probability produced by the four sequences of Eqs. (A3) versus the pulse area error α and the phase error ϵ. The first of these sequences, Eq. (A3a) clearly outperforms the others in the presence of phase errors, but still underperforms the dedicated error-correcting sequence $\Phi 5$ of Eq. (13), see Fig. 2.

[1] M. H. Levitt and R. Freeman, J. Magn. Reson. **33**, 473 (1979).
[2] R. Freeman, S. P. Kempsell, and M. H. Levitt, J. Magn. Reson. **38**, 453 (1980).
[3] M. H. Levitt, J. Magn. Reson. **48**, 234 (1982).
[4] M. H. Levitt and R. R. Ernst, J. Magn. Res. **55**, 247 (1983).
[5] M. H. Levitt, Prog. NMR Spectrosc. **18**, 61 (1986).
[6] H. M. Cho, R. Tycko, A. Pines, and J. Guckenheimer, Phys. Rev. Lett. **56**, 1905 (1986).
[7] H. Cho, J. Baum, and A. Pines, J. Chem. Phys. **86**, 3089 (1987).
[8] S. Wimperis, J. Magn. Reson. **83**, 509 (1989).
[9] S. Wimperis, J. Magn. Reson. **86**, 46 (1990).
[10] S. Wimperis, J. Magn. Reson. **109**, 221 (1994).
[11] M. H. Levitt, *Spin Dynamics: Basics of Nuclear Magnetic Resonance* (Wiley, New York, 2001).
[12] L. M. K. Vandersypen and I. L. Chuang, Rev. Mod. Phys. **76**, 1037 (2004).
[13] M. H. Levitt, in *Encyclopedia of Magnetic Resonance* (Wiley, New York, 2007), p. 1396.
[14] N. V. Vitanov, T. Halfmann, B. W. Shore, and K. Bergmann, Annu. Rev. Phys. Chem. **52**, 763 (2001).
[15] A. D. Bain, D. W. Hughes, C. K. Anand, Z. Nie, and V. J. Robertson, Magn. Reson. Chem. **48**, 630 (2010).
[16] J. Moore, M. Jankiewicz, H. Zeng, A. W. Anderson, and J. C. Gore, J. Magn. Res. **205**, 50 (2010).
[17] W. Chen, A. Takahashi, and E. Han, Magn. Res. Imaging **29**, 608 (2011).
[18] J. Moore, M. Jankiewicz, A. W. Anderson, and J. C. Gore, J. Magn. Res. **214**, 200 (2012).
[19] D. Carnevale and G. Bodenhausen, Chem. Phys. Lett. **530**, 120 (2012).
[20] G. Leung, G. Norquay, R. F. Schulte, and J. M. Wild, Magn. Res. Med. **73**, 21 (2015).
[21] M. Shen, Q. Chen, J.-P. Amoureux, and B. Hu, Solid State NMR **78**, 5 (2016).
[22] A. Brinkmann and L. A. O'Dell, Solid State NMR **84**, 34 (2017).
[23] P. Duan and K. Schmidt-Rohr, J. Magn. Res. **285**, 68 (2017).
[24] S. Odedra and S. Wimperis, J. Magn. Reson. **214**, 68 (2012).
[25] V. S. Manu and G. Veglia, J. Magn. Res. **260**, 136 (2015).
[26] Y. Xia, P. Rossi, M. V. Subrahmanian, C. Huang, T. Saleh, C. Olivieri, C. G. Kalodimos, and G. Veglia, J. Biomol. NMR **69**, 237 (2017).
[27] N. Khaneja, J. Magn. Res. **277**, 113 (2017).
[28] S. Odedra and S. Wimperis, J. Magn. Reson. **221**, 41 (2012).
[29] S. Odedra, M. J. Thrippleton, and S. Wimperis, J. Magn. Reson. **225**, 81 (2012).
[30] N. J. Clayden, S. P. Cottrell, and I. McKenzie, J. Magn. Res. **214**, 144 (2012).
[31] J. A. Jones, Prog. Nucl. Magn. Res. Spectr. **59**, 91 (2011).
[32] S. Husain, M. Kawamura, and J. A. Jones, J. Magn. Res. **230**, 145 (2013).
[33] S. Gulde, M. Riebe, G. P. T. Lancaster, C. Becher, J. Eschner, H. Häffner, F. Schmidt-Kaler, I. L. Chuang, and R. Blatt, Nature **421**, 48 (2003).
[34] F. Schmidt-Kaler, H. Häffner, M. Riebe, S. Gulde, G. P. T. Lancaster, T. Deuschle, C. Becher, C. F. Roos, J. Eschner, and R. Blatt, Nature **422**, 408 (2003).
[35] H. Häffner, C. F. Roos, and R. Blatt, Phys. Rep. **469**, 155 (2008).
[36] N. Timoney, V. Elman, S. Glaser, C. Weiss, M. Johanning, W. Neuhauser, and C. Wunderlich, Phys. Rev. A **77**, 052334 (2008).
[37] T. Monz, K. Kim, W. Hänsel, M. Riebe, A. S. Villar, P. Schindler, M. Chwalla, M. Hennrich, and R. Blatt, Phys. Rev. Lett. **102**, 040501 (2009).
[38] C. M. Shappert, J. T. Merrill, K. R. Brown, J. M. Amini, C. Volin, S. C. Doret, H. Hayden, C. S. Pai, and A. W. Harter, New J. Phys. **15**, 083053 (2013).
[39] E. Mount, C. Kabytayev, S. Crain, R. Harper, S.-Y. Baek, G. Vrijsen, S. T. Flammia, K. R. Brown, P. Maunz, and J. Kim, Phys. Rev. A **92**, 060301(R) (2015).
[40] W. Rakreungdet, J. H. Lee, K. F. Lee, B. E. Mischuck, E. Montano, and P. S. Jessen, Phys. Rev. A **79**, 022316 (2009).
[41] T. Zanon-Willette, R. Lefevre, R. Metzdorff, N. Sillitoe, S. Almonacil, M. Minissale, E. de Clercq, A. V. Taichenachev, V. I. Yudin, and E. Arimondo, Rep. Prog. Phys. **81**, 094401 (2018).
[42] D. L. Butts, K. Kotru, J. M. Kinast, A. M. Radojevic, B. P. Timmons, and R. E. Stoner, J. Opt. Soc. Am. B **30**, 922 (2013).

[43] A. Dunning, R. Gregory, J. Bateman, N. Cooper, M. Himsworth, J. A. Jones, and T. Freegarde, Phys. Rev. A **90**, 033608 (2014).
[44] P. Berg, S. Abend, G. Tackmann, C. Schubert, E. Giese, W. P. Schleich, F. A. Narducci, W. Ertmer, and E. M. Rasel, Phys. Rev. Lett. **114**, 063002 (2015).
[45] G. Demeter, Phys. Rev. A **93**, 023830 (2016).
[46] X. Wang, L. S. Bishop, J. P. Kestner, E. Barnes, K. Sun, and S. Das Sarma, Nat. Commun. **3**, 997 (2012).
[47] J. P. Kestner, X. Wang, L. S. Bishop, E. Barnes, and S. Das Sarma, Phys. Rev. Lett. **110**, 140502 (2013).
[48] X. Wang, L. S. Bishop, E. Barnes, J. P. Kestner, and S. Das Sarma, Phys. Rev. A **89**, 022310 (2014).
[49] C. Zhang, R. E. Throckmorton, X.-C. Yang, X. Wang, E. Barnes, and S. Das Sarma, Phys. Rev. Lett. **118**, 216802 (2017).
[50] G. T. Hickman, Xin Wang, J. P. Kestner, and S. Das Sarma, Phys. Rev. B **88**, 161303(R) (2013).
[51] K. Eng, T. D. Ladd, A. Smith, M. G. Borselli, A. A. Kiselev, B. H. Fong, K. S. Holabird, T. M. Hazard, B. Huang, P. W. Deelman, I. Milosavljevic, A. E. Schmitz, R. S. Ross, M. F. Gyure, and A. T. Hunter, Sci. Adv. **1**, e1500214 (2015).
[52] X. Rong, J. Geng, F. Shi, Y. Liu, K. Xu, W. Ma, F. Kong, Z. Jiang, Y. Wu, and J. Du, Nat. Commun. **6**, 8748 (2015).
[53] C. D. Aiello, M. Hirose, and P. Cappellaro, Nat. Commun. **4**, 1419 (2013).
[54] C. Ventura-Velázquez, B. J. Ávila, E. Kyoseva, and B. M. Rodriguez-Lara, Sci. Rep. **9**, 4382 (2019).
[55] B. T. Torosov and N. V. Vitanov, Phys. Rev. A **83**, 053420 (2011).
[56] G. H. Low, T. J. Yoder, and I. L. Chuang, Phys. Rev. A **89**, 022341 (2014).
[57] G. H. Low, T. J. Yoder, and I. L. Chuang, Phys. Rev. X **6**, 041067 (2016).
[58] B. T. Torosov, S. Guérin, and N. V. Vitanov, Phys. Rev. Lett. **106**, 233001 (2011).
[59] D. Schraft, T. Halfmann, G. T. Genov, and N. V. Vitanov, Phys. Rev. A **88**, 063406 (2013).
[60] F.-Q. Dou, H. Cao, J. Liu, and L.-B. Fu, Phys. Rev. A **93**, 043419 (2016).
[61] T. Ichikawa, M. Bando, Y. Kondo, and M. Nakahara, Phys. Rev. A **84**, 062311 (2011).
[62] M. Bando, T. Ichikawa, Y. Kondo, and M. Nakahara, J. Phys. Soc. Jpn. **82**, 014004 (2013).
[63] T. Ichikawa, J. G. Filgueiras, M. Bando, Y. Kondo, M. Nakahara, and D. Suter, Phys. Rev. A **90**, 052330 (2014).
[64] C. D. Hill, Phys. Rev. Lett. **98**, 180501 (2007).
[65] J. A. Jones, Phys. Rev. A **87**, 052317 (2013).
[66] J. A. Jones, Phys. Lett. A **377**, 2860 (2013).
[67] J. T. Merrill and K. R. Brown, Adv. Chem. Phys. **154**, 241 (2014).
[68] I. Cohen, A. Rotem, and A. Retzker, Phys. Rev. A **93**, 032340 (2016).
[69] F. A. Calderon-Vargas and J. P. Kestner, Phys. Rev. Lett. **118**, 150502 (2017).
[70] Y. Tomita, J. T. Merrill, and K. R. Brown, New J. Phys. **12**, 015002 (2010).
[71] X.-C. Yang, M.-H. Yung, and X. Wang, Phys. Rev. A **97**, 042324 (2018).
[72] C. Kabytayev, T. J. Green, K. Khodjasteh, M. J. Biercuk, L. Viola, and K. R. Brown, Phys. Rev. A **90**, 012316 (2014).
[73] C. D. West and A. S. Makas, J. Opt. Soc. Am. **39**, 791 (1949).
[74] M. G. Destriau and J. Prouteau, J. Phys. Radium **10**, 53 (1949).
[75] S. Pancharatnam, Proc. Ind. Acad. Sci. **41**, 130 (1955); **41**, 137 (1955).
[76] S. E. Harris, E. O. Ammann, and A. C. Chang, J. Opt. Soc. Am. **54**, 1267 (1964).
[77] C. M. McIntyre and S. E. Harris, J. Opt. Soc. Am. **58**, 1575 (1968).
[78] T. Peters, S. S. Ivanov, D. Englisch, A. A. Rangelov, N. V. Vitanov, and T. Halfmann, Appl. Opt. **51**, 7466 (2012).
[79] G. T. Genov, A. A. Rangelov, and N. V. Vitanov, J. Opt. **16**, 062001 (2014).
[80] A. A. Rangelov, N. V. Vitanov, and G. Montemezzani, Opt. Lett. **39**, 2959 (2014).
[81] G. T. Genov, D. Schraft, T. Halfmann, and N. V. Vitanov, Phys. Rev. Lett. **113**, 043001 (2014).
[82] M. Garwood and Y. Ke, J. Magn. Res. (1969) **94**, 511 (1991).
[83] B. T. Torosov and N. V. Vitanov, Phys. Rev. A **99**, 013402 (2019).
[84] R. Tycko and A. Pines, Chem. Phys. Lett. **111**, 462 (1984).
[85] R. Tycko, A. Pines, and J. Guckenheimer, J. Chem. Phys. **83**, 2775 (1985).
[86] A. J. Shaka and R. Freeman, J. Magn. Reson. **59**, 169 (1984).
[87] S. S. Ivanov and N. V. Vitanov, Opt. Lett. **36**, 7 (2011).
[88] N. V. Vitanov, Phys. Rev. A **84**, 065404 (2011).
[89] J. T. Merrill, S. C. Doret, G. Vittorini, J. P. Addison, and K. R. Brown, Phys. Rev. A **90**, 040301(R) (2014)
[90] E. Kyoseva and N. V. Vitanov, Phys. Rev. A **88**, 063410 (2013).
[91] B. T. Torosov and N. V. Vitanov, Phys. Rev. A **79**, 042108 (2009).
[92] B. T. Torosov and N. V. Vitanov, Phys. Rev. A **99**, 013424 (2019).